Supporting Information (SI)

For

Molecular mechanisms of humic acid-enhanced formation of the ordered secondary structure of a conserved catalytic domain in phytase

Xinfei Ge,[a] Wenjun Zhang, [*,a] Christine V. Putnis,[b,c] and Lijun Wang,[*,a]

[a]College of Resources and Environment, Huazhong Agricultural University, Wuhan 430070, China

[b]Institut für Mineralogie, University of Münster, 48149 Münster, Germany

[c]School of Molecular and Life Science, Curtin University, Perth 6845, Australia

Number of tables: 3

Number of figures: 9

Number of pages: 9

Table S1. Assignments of Amide I and Amide III band positions for protein or peptide secondary structures with respective to IR and Raman spectra.[1-4]

Structures	Amide I (cm^{-1})	Amide III (cm^{-1})
α-helix	1648-1657	1260-1310
Radom coil	1642-1660	1230-1260
β-sheet	1623-1641	1220-1265

Table S2. ΔG_b and corresponding fitting parameters of -COOH, NH_3^+ and CH_3 from DFS data (x_t, distance to transition between bound and unbound states; f_{eq}, equilibrium force). All values are represented as mean ± standard deviation.

Solutions	Surfaces	Functional groups	*k* (N/m)	Fitting parameters		$-\Delta G_b$ (KJ/mol)
				x_t (Å)	f_{eq} (pN)	
without phytate	mica	COOH	0.1012	0.82±0.066	230.53±14.20	17.42±1.98
		NH_3^+	0.1078	0.90±0.052	165.19±12.04	14.56±1.65
		CH_3	0.0965	0.61±0.042	82.68 ± 7.49	6.45 ± 0.83
	HA	COOH	0.0921	0.90±0.088	189.04±12.46	16.17±1.75
		NH_3^+	0.1105	0.91±0.034	251.98±15.89	21.76±2.62
		CH_3	0.0791	0.64±0.055	90.45±7.84	6.55±0.96
with phytate	mica	COOH	0.0872	0.74±0.048	239.20±19.14	16.78±1.76
		NH_3^+	0.0932	0.72±0.052	157.61±8.90	12.13±1.53
		CH_3	0.0784	0.75±0.053	84.12±6.04	7.32±0.78
	HA	COOH	0.0694	0.73±0.064	193.87±13.19	14.45±1.86
		NH_3^+	0.0943	0.85±0.047	238.84±16.24	19.10±1.54
		CH_3	0.0847	0.62±0.067	87.28 ± 7.94	6.93 ± 0.82

Table S3. ΔG_b and corresponding fitting parameters of ACD, ACD-1 and ACD-2 from DFS data (x_t, distance to transition between bound and unbound states; f_{eq},

equilibrium force). All values are represented as mean ± standard deviation.

Solutions	Surfaces	Active domains	k (N/m)	Fitting parameters		$-\Delta G_b$
				x_t (Å)	f_{eq} (pN)	(KJ/mol)
without phytate	mica	ACD	0.0915	0.54±0.044	95.52±6.07	6.14±0.55
		ACD-1	0.0786	0.60±0.045	86.17±7.28	6.13±0.88
		ACD-2	0.0623	0.63±0.032	90.14±6.47	6.23±0.67
	HA	ACD	0.0831	0.77±0.086	203.59±14.3	15.71±1.2
		ACD-1	0.0905	0.59±0.038	91.49±8.49	6.38±0.51
		ACD-2	0.0718	0.64±0.057	204.78±14.2	14.8±1.57
with phytate	mica	ACD	0.0859	0.66±0.047	167.31±9.65	11.64±0.63
		ACD-1	0.0672	0.71±0.052	87.04±9.12	7.20±0.60
		ACD-2	0.0826	0.53±0.062	87.54±6.89	6.37±0.72
	HA	ACD	0.0799	0.88±0.054	231.26±13.14	19.29±1.94
		ACD-1	0.1043	0.59±0.057	94.74±8.16	6.58±0.96
		ACD-2	0.0619	0.74±0.057	96.45±12.2	6.7±0.88

Full-length phytase (FLP):

MSDMKSGNIS **RHGVRAP**PFL SLLIPLTPQS AFAQSEPELK

LESVVIVSMK AILITKATQL MQDVTPDAWP TWPVKLGWLT

PRGGELIAYL GHYQRQRLVA DGLLTKKGCP QPGQVAIIAD

VDERTRKTGE AFAAGLAPDC AISVHTQADT SSPDPLFNPL

KTGVCQLDNA NVTDAILSRA GGSIADFTGH RQTAFRELER

VLNFPQSNLC LNREKQDESC SLTQALPSEL KVSADNVSLT

GAVSLASMLT EIFLLQ**HD**QG MPEPGGEGSP IHTSGTPC

Fig. S1. Amino acid sequences of FLP (Origin: EC 3.1.3.26, *Escherichia coli*) containing N-terminal (RHGVRAP, ACD-1) and C-terminal (HD) active domains.

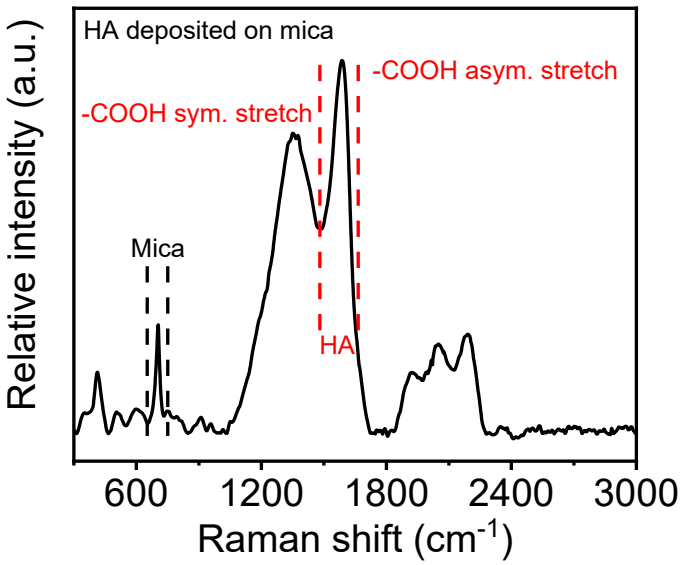

47

48 **Fig. S2**. Raman characteristic vibrations of mica and HA selected to conduct Raman

49 mapping.

50

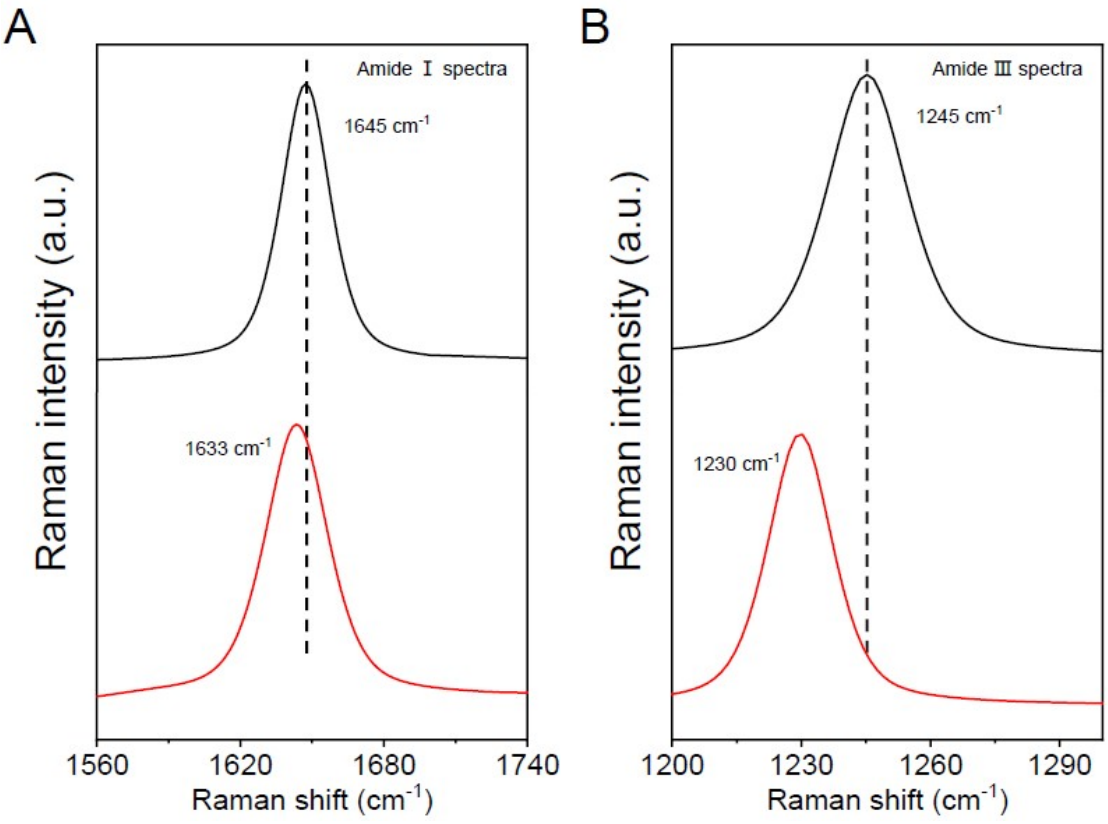

51

Fig. S3. Secondary structures of ACD in the region of (A) Amide I and (B) Amide III before (black lines) and after (red lines) treatment with HA.

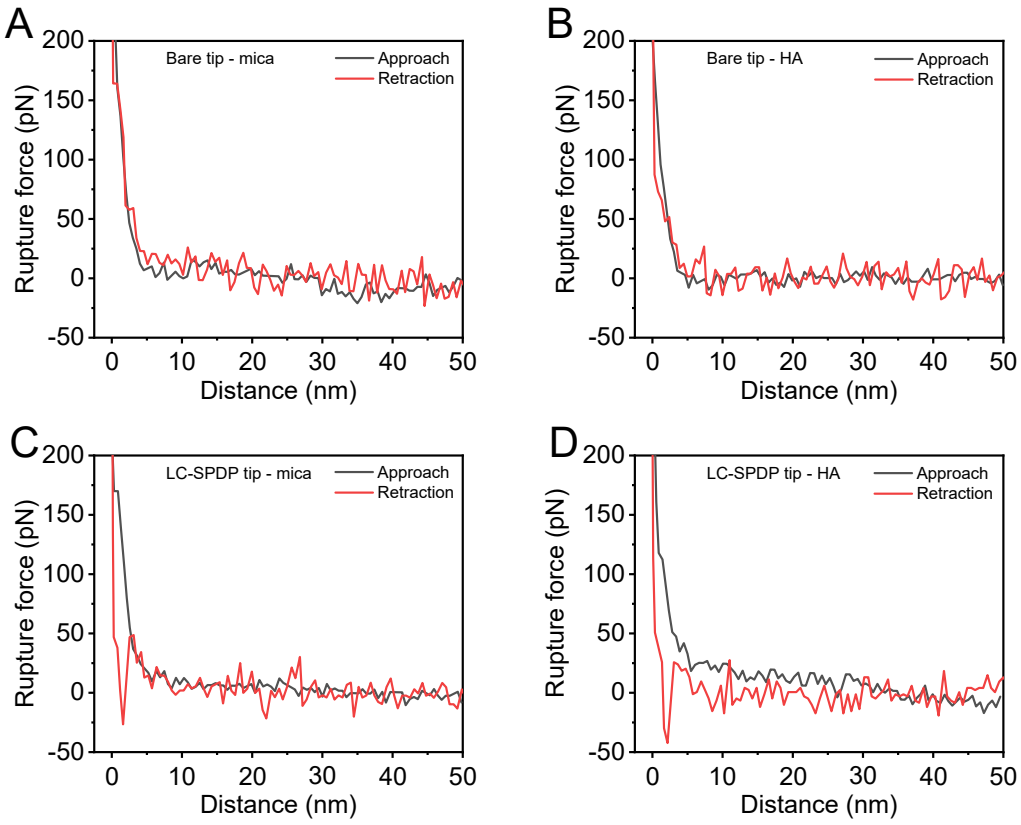

Fig. S4. Representative F-D curves between the Au-coated bare tip with (A) mica and (B) HA surface. Representative F-D curves between the LC-SPDP-functionalized tip with (C) mica and (D) HA surface. These typical F-D curves as key controls collectively excluded the interference from the interaction between Au-coated or LC-SPDP-functionalized tips and the two surfaces compared to functionalized tips of ACD(-1/2) as well as -CH_3-, -COOH-, -NH_3-terminal organic molecules.

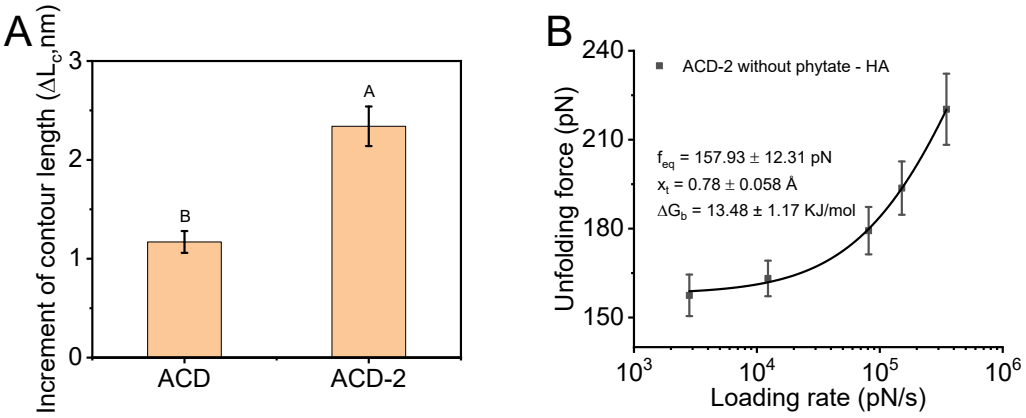

61

62 **Fig. S5.** (A) Analyses of ΔL_c of ACD and ACD-2 separated from HA deposited on

63 mica surface. Different uppercase letters indicate significant difference at $P < 0.01$,

64 which was analyzed by SPSS software. (B) A plot of mean unfolding force of the first

65 force-peak occurred in double-force curves versus loading rates, determining f_{eq} and

66 ΔG_b for allowing to break H-bonding as ACD-2 is retracted from HA. The derived f_{eq}

67 and ΔG_b are presented as mean ± standard deviations ($n = 3$).

68

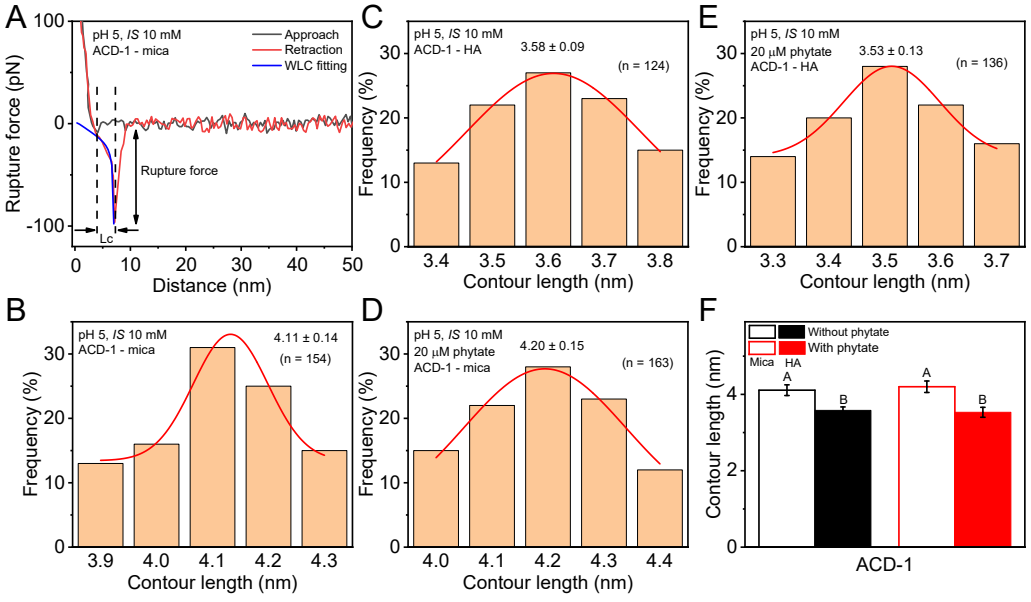

69

70 **Fig. S6.** (A) Representative F-D curve between ACD-1 and mica fitted by the WLC

model. The contour length (L_c) obtained from F-D curves through WLC fitting during detaching ACD-1 from (B, D) mica and (C, E) mica with adsorbed HA in solutions (pH 5 and *IS* = 10 mM NaCl) in the absence and presence of 20 μM phytate. (F) Analysis of L_c of ACD-1 separated from mica or mica with adsorbed HA. Different uppercase letters indicate significant difference at $P < 0.01$, which was analyzed by SPSS software.

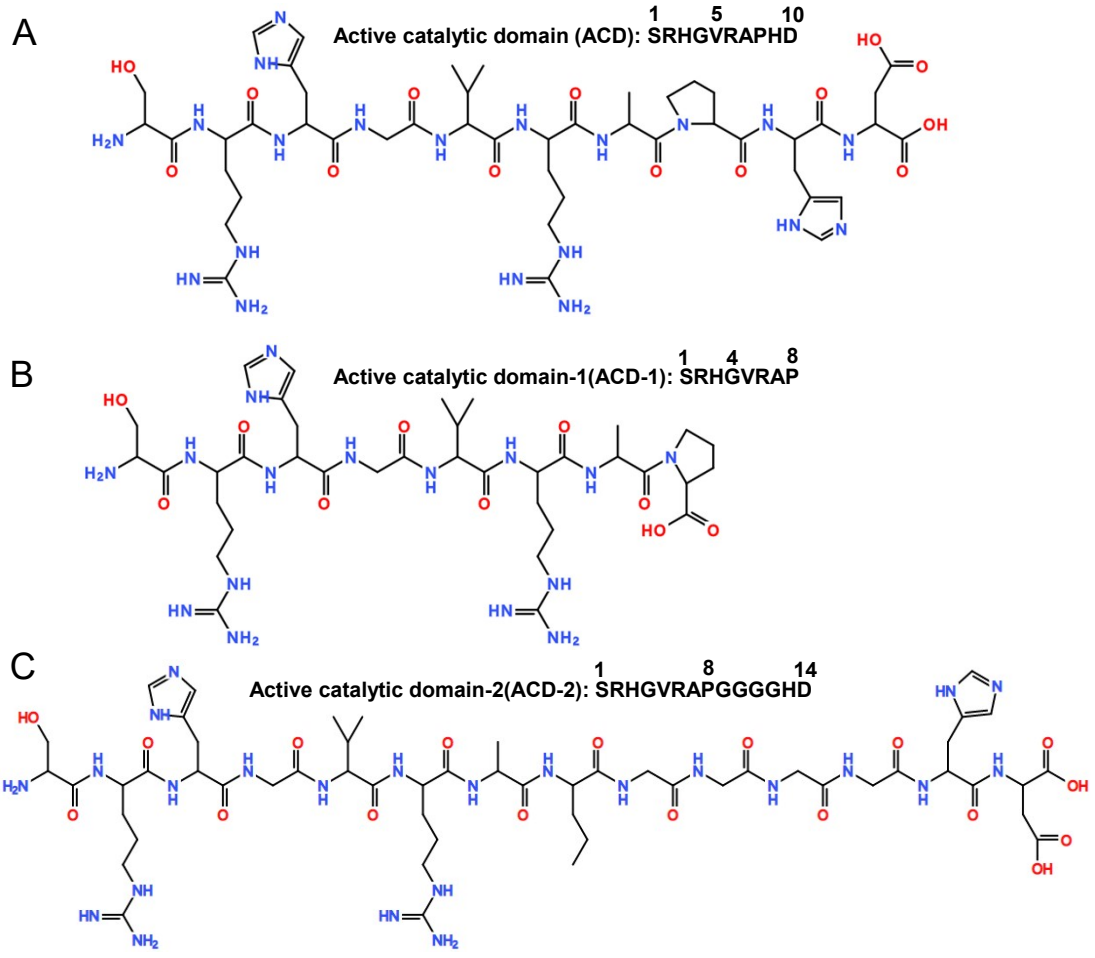

Fig. S7. Chemical structures of (A) ACD, (B) ACD-1 and (C) ACD-2 showing representative chemistries containing CH_3, NH_3^+ and COOH.

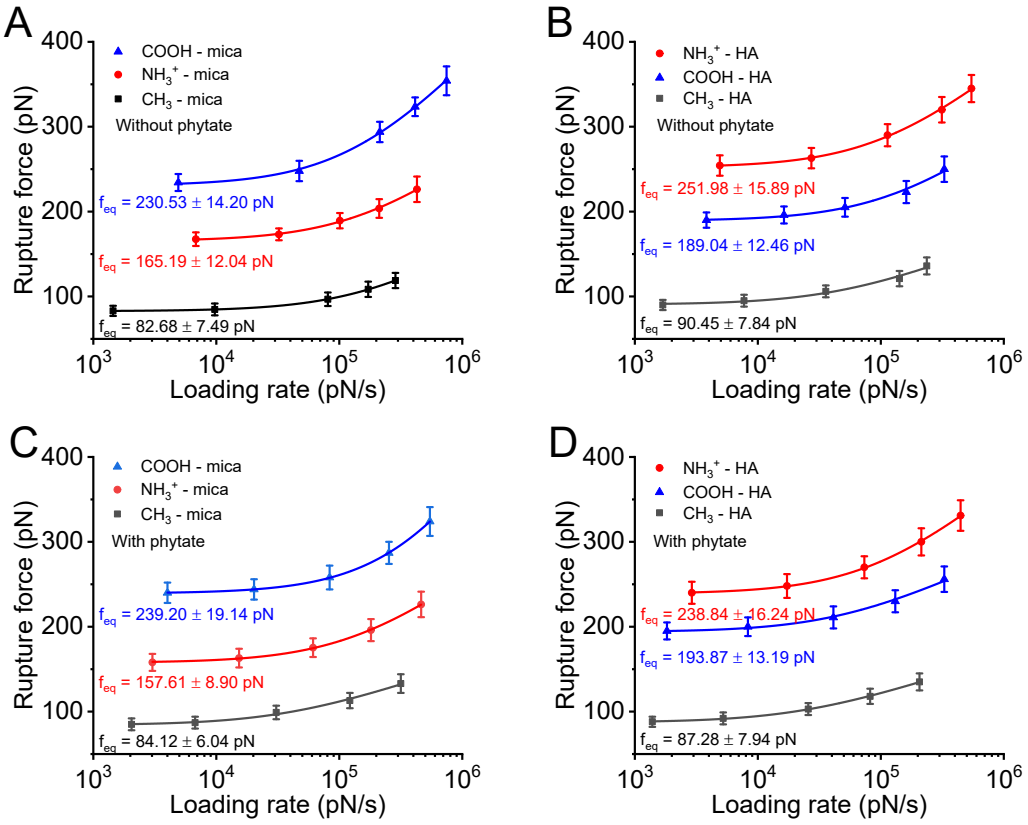

Fig. S8. Plots of mean rupture forces versus loading rates of COOH-, NH_3^+- or CH_3-terminal model organic molecule at the mica/HA interface in the (A, B) absence and (C, D) presence of 20 μM phytate in solutions (pH 5 and *IS* 10 mM NaCl).

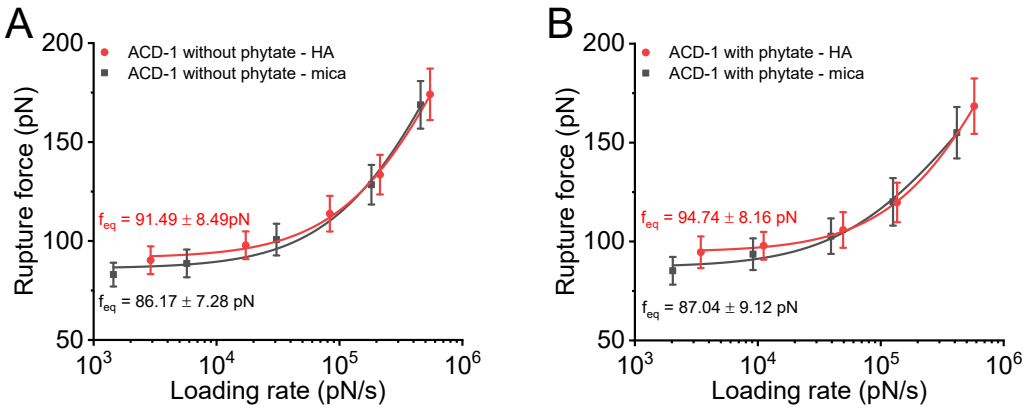

Fig. S9. Plots of mean rupture forces versus loading rates of ACD-1 at the mica/HA interface in the (A) absence and (B) presence of 20 μM phytate in solutions (pH 5 and *IS* 10 mM).

SI References

1 A. Barth and C. Zscherp, What Vibrations Tell Us about Proteins. *Quar. Rev. Biophys.*, 2002, **35**, 369-430.

2 L. Tamm and S. A. Tatulian, Infrared spectroscopy of proteins and peptides in lipid bilayers. *Quar. Rev. Biophys.*, 1997, **30**, 365-429.

3 G. Vedantham, H. G. Sparks, S. U. Sane, S. Tzannis and T. M. Przybycien, A holistic approach for protein secondary structure estimation from infrared spectra in H_2O solutions. *Anal. Biochem.*, 2000, **285**, 33-49.

4 E. A. Cooper and K. Knutson, Fourier transform infrared spectroscopy investigations of protein structure. *Pharm. Biotechnol.*, 1995, **7**, 101-143.